Journal of Applied Mechanics Vol.12, pp.729-735 (August 2009) JSCE

Study of intertia-region characteristics of dam break flow of finite extent.

How Tion PUAY* and Takashi HOSODA**

*PhD Student Dept. Urban Management, Kyoto Univ.
(Kyodai Katsura, Nishikyo-ku, Kyoto 615-8530)
**Member of JSCE, Professor, Dept. Urban Management, Kyoto Univ.
(Kyodai Katsura, Nishikyo-ku, Kyoto 615-8530)

Characteristics of inertia flow generated from the release of inviscid fluid behind a dam with finite extent in a semi-infinitely long, initially dry channel are examined. Analytical solutions of the flow in the whole domain from the moment the flow is initiated are derived. Comparison with a depth averaged numerical model is carried out.

Key Words : *inertia region, inviscid*

1. Introduction

Dam break flows have been intensively studied, analytically and experimentally, as model of actual dam break failure and associated effects such as surging wave and debris flow. The study of dam break flow has also been used to evaluate rheological properties of fresh concrete, e.g. a slump flow test being treated as a kind of dam break flow [1)].

In the author's previous work [2)], temporal attenuation of depth at the origin and propagation of wave front are used as parameters to define the inertia and viscous region characteristics. A simple solution defining the profile of the flow depth near the origin is obtained. However this solution is only applicable in the region very close to the origin, and inadequate to fully define the profile further away from the origin.

2. Theoretical Analysis

2.1 Governing equations

The flow from a sudden release of inviscid fluid in a dam can be adequately described by the following one-dimensional depth averaged continuity and momentum equations as follows,

$$\frac{\partial h}{\partial t} + \frac{\partial hU}{\partial x} = 0 \tag{1}$$

$$\frac{\partial hU}{\partial t} + \frac{\partial hU^2}{\partial x} + gh\frac{\partial h}{\partial x} = \frac{\tau_b}{\rho} \tag{2}$$

with h as the depth of flow, U as the flow velocity in x direction, ν as the kinematic viscosity, ρ as the fluid density, τ_b as the bottom shear stress and g as the gravity acceleration. Schematic of dam break flow of finite extent is shown in Fig.1, where h_m is the depth at the origin, L is the wave front position from the origin, L_o and h_o are initial width and height of the dam respectively .

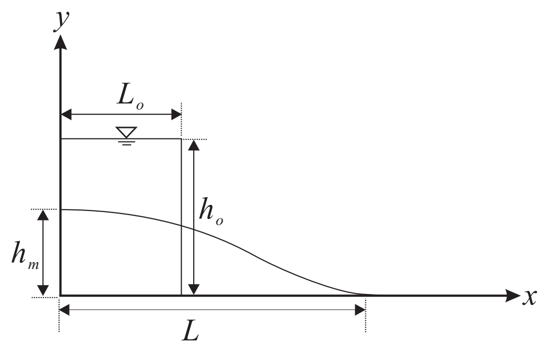

Fig. 1 Dam break flow of finite volume.

2.2 Theoretical formulation

The characteristic lines defining the kinematics of flow in the dam break flow of finite-extent are shown in Fig.2 . Immediately after the flow is initiated by the release of fluid in the dam, the initial positive characteristic line will travel downstream, while the initial negative characteristic line will propagate upstream toward the wall at the origin. The time taken for the negative wave to reach the upstream wall is defined as t_o,

$$t_o = \frac{L_o}{c_o} \tag{3}$$

where c_o is the wave celerity defined as $\sqrt{gh_o}$. The analytical solution for the propagation of wave front, L due to the release of fluid behind an infinite extent dam can be obtained [3)] and the solution is given by

$$L = L_o + 2\sqrt{gh_o}t \tag{4}$$

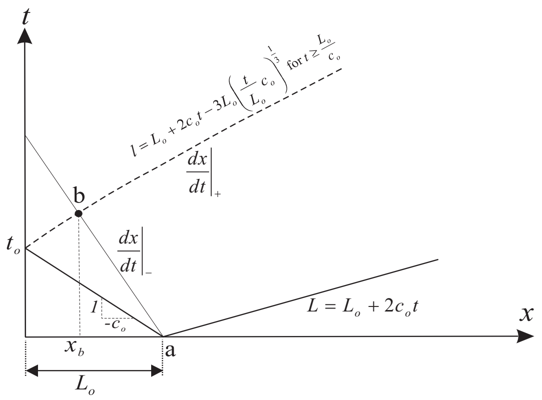

Fig. 2 Characteristic lines of dam break flow of finite volume.

The position of the first negative wave reflected by the upstream wall, (represented by dotted line in Fig.2), can be determined by solving $l(t)$, which is the position of point b, by using characteristic line, [4] and the solution is given by

$$l(t) = L_o + 2c_o t - 3L_o\left(\frac{c_o t}{L_o}\right)^{\frac{1}{3}} \tag{5}$$

The velocity at b can be calculated as:

$$U_b(t) = 2c_o - 2c_o\left(\frac{c_o t}{L_o}\right)^{-\frac{2}{3}} \tag{6}$$

By comparing Eq.(4) and Eq.(5), it is noted that the first negative wave reflected by the upstream wall always trail behind the front wave. Hence, in this study, an approach of dividing the flow into 2 regions is made. The first region, named Region A hereafter, is the region preceding the first negative wave, undisturbed by the negative wave reflected from the upstream wall, traveling downstream, and remains analogous to the flow in dam break flow of infinite extent. The second region, named Region B hereafter, is the region trailing behind the first negative wave. Region A is shown in Fig.3 (a) while both Region A and B are shown in Fig.3 (b). It is worth noting that Region B starts from $t > t_o$.

(1) Solution of region A

Region A is analogous to the flow of dam break flow of infinite extent. The solution for the depth in this region is given as [3]:

$$h_2(x,t) = \frac{1}{9g}\left(2\sqrt{gh_o} - \frac{x - L_o}{t}\right)^2 \tag{7}$$

(2) Solution of region B

The depth of flow h and flow velocity U in region B are expressed in the following power series:

$$h_2(t) = h_m(t) + a_1(t)\left(\frac{x}{h_o}\right) + a_2(t)\left(\frac{x}{h_o}\right)^2 + a_3(t)\left(\frac{x}{h_o}\right)^3 + a_4(t)\left(\frac{x}{h_o}\right)^4 + \ldots \tag{8}$$

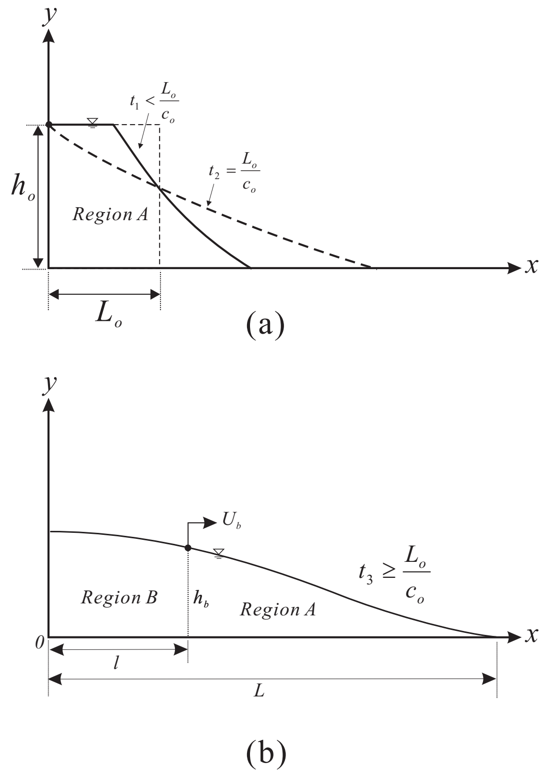

Fig. 3 Dam break flow of finite volume.

$$U(t) = \sqrt{gh_o}\left[b_1(t)\left(\frac{x}{h_o}\right) + b_2(t)\left(\frac{x}{h_o}\right)^2 + b_3(t)\left(\frac{x}{h_o}\right)^3 + b_4(t)\left(\frac{x}{h_o}\right)^4 + \ldots\right] \tag{9}$$

where h_o = representative flow depth, x = distance from the origin, $a_1(t)$, $a_2(t)$, $a_3(t)$, $a_4(t)$, $b_1(t)$, $b_2(t)$, $b_3(t)$, and $b_4(t)$ are time dependent coefficients while other parameters are defined as in Fig.1. By substituting the power series of h and U into the continuity and momentum equations in Eq.(1) and Eq.(2), we can rewrite both equations again by order of power as in the following equations :

Continuity Equation:

0th order

$$\frac{dh_m}{dt} + \sqrt{gh_o}\frac{h_m b_1}{h_o} = 0 \tag{10}$$

1st, 2nd and 3rd order

$$\frac{1}{{h_o}^2}\frac{da_n}{dt} + \frac{\sqrt{gh_o}}{{h_o}^{n+1}}\left[(n+1)h_m b_{n+1} + \sum_{j=1}^{n}(n+1)a_j b_{n-j+1}\right] = 0 \tag{11}$$

where n = 1,2 and 3 for 1^{st}, 2^{nd} and 3^{rd} order respectively. Since U is expanded up to the order of 4 in the Taylor's series, the term $(n+1)h_m b_{n+1}$ is neglected in the case of the 4^{th} order.

Momentum equation:
0th order

$$\frac{gh_m^2 a_1}{h_o} = 0 \tag{12}$$

1st order

$$\frac{\sqrt{gh_o}}{h_o} h_m \frac{d}{dt}\left(h_m b_1\right) + \frac{g}{h_o}\left(2h_m^2 b_1^2\right) + \frac{g}{h_o^2}\left(2a_2 h_m^2 + 2h_m a_1^2\right) = -3\nu\sqrt{gh_o}\frac{b_1}{h_o} \tag{13}$$

2nd order

$$\frac{\sqrt{gh_o}}{h_o^2}\left[h_m \frac{d}{dt}\left(h_m b_2 + a_1 b_1\right) + a_1 \frac{d}{dt}\left(h_m b_1\right)\right] + \frac{g}{{h_o}^2}\left(6b_1 b_2 h_m^2 + 5h_m a_1 b_2^2\right) + \frac{g}{h_o^3}\left[3a_3 h_m^2 + 4h_m a_1 a_2 + a_1\left(a_1^2 + 2a_2 h_m\right)\right] = -3\nu\sqrt{gh_o}\frac{b_2}{h_o^2} \tag{14}$$

3rd order

$$\frac{\sqrt{gh_o}}{h_o^3}\left[h_m \frac{d}{dt}\left(h_m b_3 + a_1 b_2 + a_2 b_1\right) + \frac{a_1}{h_o^3}\frac{d}{dt}\left(h_m b_2 + a_1 b_1\right) + \frac{a_2}{h_o^3}\frac{d}{dt}\left(h_m b_1\right)\right] + \frac{g}{h_o^3}\left[8b_1 b_3 h_m^2 + 6h_m a_2 b_1^2 + 4b_2^2 h_m^2 + 8b_1 b_2 h_m + 6a_1 b_1 b_2 h_m + 3a_1 b_1^2\right] + \frac{g}{h_o^4}\left[4a_4 h_m^2 + 6h_m a_1 a_3 + 2a_2\left(a_1^2 + 2a_2 h_m\right) + a_1\left(2a_3 h_m + 2a_1 a_2\right)\right] = -3\nu\sqrt{gh_o}\frac{b_3}{h_o^3} \tag{15}$$

In the case of invisic fluid, $\nu = 0$. We can deduce from Eq.(12) that $a_1 = 0$. Therefore from Eq.(11), we have $b_2 = 0$. Consequently, from Eq.(14) and Eq.(11), we can further deduce $a_3 = 0$ and $b_4 = 0$. The h and U series can therefore be expressed as:

$$h\left(t\right) = h_m\left(t\right) + a_2\left(t\right)\left(\frac{x}{h_o}\right)^2 + a_4\left(t\right)\left(\frac{x}{h_o}\right)^4 + \ldots \tag{16}$$

$$U\left(t\right) = \sqrt{gh_o}\left[b_1\left(t\right)\left(\frac{x}{h_o}\right) + b_3\left(t\right)\left(\frac{x}{h_o}\right)^3 + \ldots\right] \tag{17}$$

2.3 Moving Coordinate Formulation

In order to further improve the formulation of the author's previous work [2)], which is only adequate to express the profile near to the origin, a new formulation based on a moving coordinate system is introduced here. A moving coordinate system ξ which is based on the propagation of the first negative wave, hereafter, referred as point b, is as follows:

$$\xi = \frac{x}{l(t)} \tag{18}$$

Continuity and momentum equations as in Eq.(1) and Eq.(2) expressed in ξ coordinate systems are therefore:

$$\frac{\partial h}{\partial t} - \xi\frac{dl}{dt}\frac{\partial h}{\partial \xi} + \frac{h}{l}\frac{\partial U}{\partial \xi} + \frac{U}{l}\frac{\partial h}{\partial \xi} = 0 \tag{19}$$

$$\frac{\partial U}{\partial t} - \xi\frac{dl}{dt}\frac{\partial U}{\partial \xi} + \frac{U}{l}\frac{\partial U}{\partial \xi} + \frac{g}{l}\frac{\partial h}{\partial \xi} = 0 \tag{20}$$

Based on the results in Eq.(16) and Eq.(17), the depth of flow h, and velocity U, are assumed to be expressible as a series of power expanded from point b, applicable only in Region B. By using the Taylor's power series expansion, they can be written as in Eq.(21) and Eq.(22) respectively.

$$h(t,\xi) = a_o(t) + a_2(t)\xi^2 + a_4(t)\xi^4 + \ldots \tag{21}$$

$$U(t,\xi) = b_1(t)\xi + b_3(t)\xi^3 + \ldots \tag{22}$$

Continuity Equations :
0th order :

$$l\frac{da_o}{dt} + a_o b_1 = 0 \tag{23}$$

1st order : *no equation*
2nd order :

$$l\frac{da_2}{dt} - 2a_2\frac{dl}{dt} + 2b_1 a_2 + 3a_o b_3 = 0 \tag{24}$$

3rd order : *no equation*
4th order :

$$l\frac{da_4}{dt} - 4a_4\frac{dl}{dt} + 4b_1 a_4 + 2a_2 b_3 + a_4 b_1 + 3a_2 b_3 = 0 \tag{25}$$

Momentum Equations :
0th order : *no equation*
1st order :

$$l\frac{db_1}{dt} - b_1\frac{dl}{dt} + b_1^2 + 2ga_2 = 0 \tag{26}$$

2nd order : *no equation*
3rd order :

$$l\frac{db_3}{dt} - 3b_3\frac{dl}{dt} + b_1 b_3 + 3b_1 b_3 + 4ga_4 = 0 \tag{27}$$

4th order : *no equation*

The coefficients of a_0, a_2, b_1 can be expressed as in the following series :

$$a_0(t) = a_{01}\left(\frac{t}{t_o}\right)^{-\frac{1}{3}} + a_{02}\left(\frac{t}{t_o}\right)^{-\frac{2}{3}} + a_{03}\left(\frac{t}{t_o}\right)^{-1} + a_{04}\left(\frac{t}{t_o}\right)^{-\frac{4}{3}} \quad (28)$$

$$a_2(t) = a_{20}(t) + a_{21}\left(\frac{t}{t_o}\right)^{-\frac{1}{3}} + a_{22}\left(\frac{t}{t_o}\right)^{-\frac{2}{3}} + a_{23}\left(\frac{t}{t_o}\right)^{-1} + a_{24}\left(\frac{t}{t_o}\right)^{-\frac{4}{3}} \quad (29)$$

$$b_1(t) = b_{10}(t) + b_{11}\left(\frac{t}{t_o}\right)^{-\frac{1}{3}} + b_{12}\left(\frac{t}{t_o}\right)^{-\frac{2}{3}} + b_{13}\left(\frac{t}{t_o}\right)^{-1} + b_{14}\left(\frac{t}{t_o}\right)^{-\frac{4}{3}} \quad (30)$$

As $t \to t_o$, $l \to 0$. Hence, $\xi \to \infty$. Therefore, the following conditions must be satisfied :

$$a_0(t_o) = \sum_{n=1}^{4} a_{0n} = h_0 \quad (31)$$

$$a_2(t_o) = \sum_{n=0}^{4} a_{2n} = 0 \quad (32)$$

$$b_1(t_o) = \sum_{n=0}^{4} b_{1n} = 0 \quad (33)$$

$$b_3(t_o) = 0 \quad (34)$$

By substituting Eq.(28), Eq.(29) and Eq.(30) into h and U series, and thereafter, into continuity and momentum equations in Eq.(19) and Eq.(20), a set of equations grouped based on the order of $\left(\frac{t}{t_o}\right)$ can be obtained as follows :

From Eq.(23)

$-\frac{1}{3}$ order :

$$-\frac{2}{3}a_{01}c_o + a_{01}b_{10} = 0 \quad (35)$$

$-\frac{2}{3}$ order :

$$-\frac{4}{3}a_{02}c_o + a_{01}b_{11} + a_{02}b_{10} = 0 \quad (36)$$

-1 order :

$$-2a_{03}c_o + a_{01}c_o + a_{01}b_{12} + a_{02}b_{11} + a_{03}b_{10} = 0 \quad (37)$$

$-\frac{4}{3}$ order :

$$-\frac{1}{3}a_{01}c_o - \frac{8}{3}a_{04}c_o + 2a_{02}c_o + a_{01}b_{13} + a_{02}b_{12} + a_{03}b_{11} + a_{04}b_{10} = 0 \quad (38)$$

From Eq.(26)

0 order :

$$-2c_ob_{01} + {b_{10}}^2 + 2ga_{20} = 0 \quad (39)$$

$-\frac{1}{3}$ order :

$$-\frac{2}{3}c_ob_{11} - 2c_ob_{11} + 2b_{10}b_{11} + 2ga_{21} = 0 \quad (40)$$

$-\frac{2}{3}$ order :

$$-\frac{4}{3}c_ob_{12} - 2c_ob_{12} + c_ob_{10} + {b_{11}}^2 + 2b_{10}b_{12} + 2ga_{22} = 0 \quad (41)$$

-1 order :

$$-2c_ob_{13} - c_ob_{11} - 2c_ob_{13} + c_ob_{11} + 2b_{10}b_{13} + 2b_{11}b_{12} + 2ga_{23} = 0 \quad (42)$$

$-\frac{4}{3}$ order :

$$-\frac{1}{3}c_ob_{11} - \frac{8}{3}c_ob_{14} + 2c_ob_{12} - 2c_ob_{14} + c_ob_{12} \; {b_{12}}^2 + 2b_{10}b_{14} + 2b_{11}b_{13} + 2ga_{24} = 0 \quad (43)$$

From Eq.(24)

$-\frac{1}{3}$ order :

$$-\frac{2}{3}c_oa_{21} - 4c_oa_{21} + 2\left(a_{20}b_{11} + a_{21}b_{10}\right) = 0 \quad (44)$$

$-\frac{2}{3}$ order :

$$-\frac{4}{3}c_oa_{22} - 2c_o\left(2a_{22} - a_{20}\right) + 2(a_{20}b_{12} + a_{21}b_{11} + a_{22}b_{10}) + 6c_oa_{02} - 6a_{02}b_{10} - a_{01}b_{11} = 0 \quad (45)$$

-1 order :

$$-2c_oa_{23} + c_oa_{21} - 2c_o\left(2a_{23} - a_{21}\right) + 2\left(a_{20}b_{13} + a_{21}b_{12} + a_{22}b_{11} + a_{23}b_{10}\right) + 3\left(2c_oa_{03} - a_{03}b_{10} - a_{02}b_{11} - a_{01}b_{12}\right) = 0 \quad (46)$$

$-\frac{4}{3}$ order :

$$-\frac{1}{3}c_oa_{21} - \frac{8}{3}c_oa_{24} - 2c_oa_{22} - 2c_o\left(2a_{24} - a_{22}\right) + 2\left(a_{20}b_{14} + a_{21}b_{13} + a_{22}b_{12} + a_{23}b_{11} + a_{24}b_{10}\right) + 3(2c_oa_{04} - a_{04}b_{10} - 2c_oa_{02} - a_{03}b_{11} - a_{02}b_{12} - a_{01}b_{13}) = 0 \quad (47)$$

By solving simultaneous equations of Eq.(31) to Eq.(47), the following solutions are obtained:
Coefficient of $a_o(t)$

$$a_{01} = a_{02} = a_{04} = 0$$
$$a_{03} = h_o,$$
$$\therefore a_0(t) = h_o\left(\frac{t}{t_o}\right)^{-1} \quad (48)$$

Coefficient of $a_2(t)$

$$a_{20} = a_{21} = a_{22} = a_{23} = a_{24} = 0$$
$$\therefore a_2(t) = 0 \quad (49)$$

Coefficient of $b_1(t)$

$$b_{11} = b_{14} = 0$$
$$b_{12} = -3c_o, \quad b_{13} = c_o, \quad b_{10} = 2c_o$$
$$\therefore b_1(t) = 2c_o - 3c_o\left(\frac{t}{t_o}\right)^{-\frac{2}{3}} + c_o\left(\frac{t}{t_o}\right)^{-1} \quad (50)$$

At $x = l$, $\xi = 1$,

$$a_0(t) + a_2(t) + a_4(t) = h_b = h_o\left(\frac{t}{t_o}\right)^{-\frac{4}{3}} \quad (51)$$

$$b_1(t) + b_3(t) = u_b = 2c_o - 2c_o\left(\frac{t}{t_o}\right)^{-\frac{2}{3}} \quad (52)$$

By utilizing Eq.(51) and Eq.(52), $a_4(t)$ and $b_3(t)$ can be obtained as follows:

$$a_4(t) = h_o\left(\frac{t}{t_o}\right)^{-\frac{4}{3}} - h_o\left(\frac{t}{t_o}\right)^{-1} \quad (53)$$

$$b_3(t) = c_o\left(\frac{t}{t_o}\right)^{-\frac{2}{3}} - c_o\left(\frac{t}{t_o}\right)^{-1} \quad (54)$$

The depth and velocity profile for region B can be summarized as follows:

$$h_2(t,\xi) = h_o\left(\frac{t}{t_o}\right)^{-1} + \left[h_o\left(\frac{t}{t_o}\right)^{-\frac{4}{3}} - h_o\left(\frac{t}{t_o}\right)^{-1}\right]\xi^4 \quad (55)$$

$$U(t,\xi) = \left[2c_o - 3c_o\left(\frac{t}{t_o}\right)^{-\frac{2}{3}} + c_o\left(\frac{t}{t_o}\right)^{-1}\right]\xi + \left[c_o\left(\frac{t}{t_o}\right)^{-\frac{2}{3}} - c_o\left(\frac{t}{t_o}\right)^{-1}\right]\xi^3 \quad (56)$$

Table 1 Initial conditions of simulation for inviscid fluid.

Model	$h_o(m)$	$L_o(m)$	$\nu(m^2s^{-1})$
Depth Averaged Model	0.5	0.5	0.0

3. Numerical Simulation

3.1 Numerical Model

A depth averaged model with Harten's TVD (Total Variation Diminishing) scheme is used to solve the governing equations numerically. Two sets of spatial spacing in flow direction, dx and time step, dt are used in the model: $dx = 0.005m$ with $dt = 0.0002s$ and $dx = 0.001m$ with $dt = 0.0002s$. Depth of flow at time interval $t = 0.05s$, $t = 0.5s$ and $t = 1.0s$ are plotted.

3.2 Simulation Procedures

The flow from dam break of finite extent are simulated in a semi-infinitely long channel, with boundary wall at the origin, $x = 0$. The channel ahead of the fluid is initially dry. The size of the dam is set to $h_o = 0.5m$ by $L_o = 0.5m$. Flow is generated by instantaneously releasing the fluid in the dam. Viscosity is set to 0 for inviscid case. During the simulation, temporal variation of depth at the origin, h_m is observed. The attenuation of h_m is plotted in log axes graph. Initial conditions of the simulation are summarized in Table 1.

In order to validate the depth averaged numerical model, the propagation of the wave front is verified with the analytical solution provided in Eq.(4). The result is plotted in Fig.4 and shows good agreement between the depth averaged numerical model and the analytical solution in the case of the wave front propagation. The numerical model also shows satisfactory mass conservation, as shown in Fig.5.

3.3 Numerical Simulation Results and Discussion

The numerical results from depth averaged model and analytical solution for the flow are plotted in Fig.6 for $t = 0.5s$ and $t = 1.0s$. Analytical solution of h_1 which is valid only in Region A agrees satisfactorily with the profile obtained from the depth averaged model. This is because the depth averaged model is solving the same governing equations which the analytical solution of h_1 is derived. The results of the analytical solution of h_2, however shows that the flow depth does not match the numerical model result accurately. However the discrepancy between the analytical solution h_2 and the numerical model reduces as the flow propagates further downstream. For the

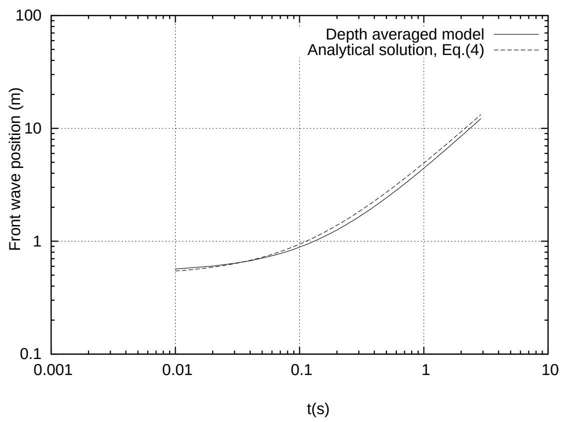

Fig. 4 Temporal variation of wave front L_m for depth averaged model and analytical solution.

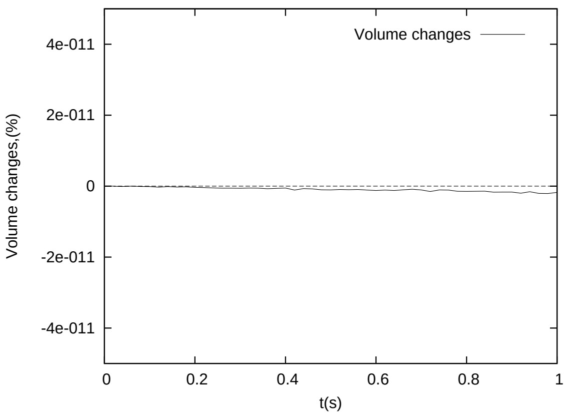

Fig. 5 Volume changes with time for depth averaged model.

attenuation of depth at the origin, the result is plotted in Fig.7. In the author's previous work [2)], the attenuation of depth at the origin is found to be inversely proportionate with time ($h_m \propto t^{-1}$). It can be seen from Fig.7 that the analytical solution $h_2(t)$ agrees satisfactorily with the slope, $m = -1$.

It is worth to note that another flow characteristics can be observed in Region A and Region B as shown in Fig.8. The Froude number at position b ($t = t_o$) in Fig.2 is calculated as follows :

$$Fr = \frac{U'}{c_o} = \frac{\frac{dl}{dt} - U_b}{c_o} = 1 \tag{57}$$

Therefore, position b, which is the position of the first negative wave reflected by the upstream boundary wall, is an important point that defines the boundary of Region A where the flow is supercritical and Region B where the flow is subcritical. The existence of subcritical flow in Region B means that analytical solution is obtainable by considering boundary conditions at one upstream point and one downstream point in Region B, which is used as the basis of the analytical formulation in this study.

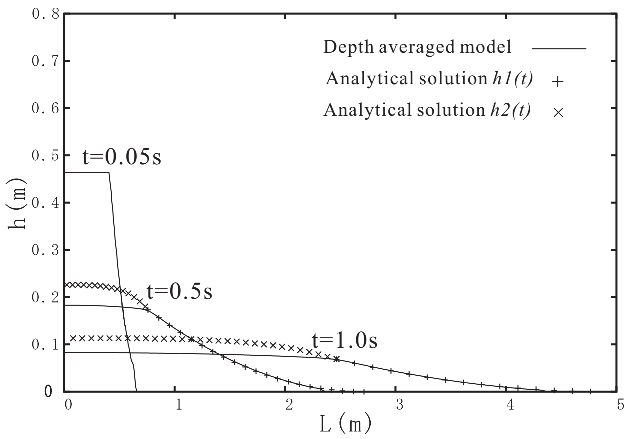

Fig. 6 Profile of dam break flow of inviscid fluid using depth averaged model and analytical solutions of $h_1(t)$ and $h_2(t)$

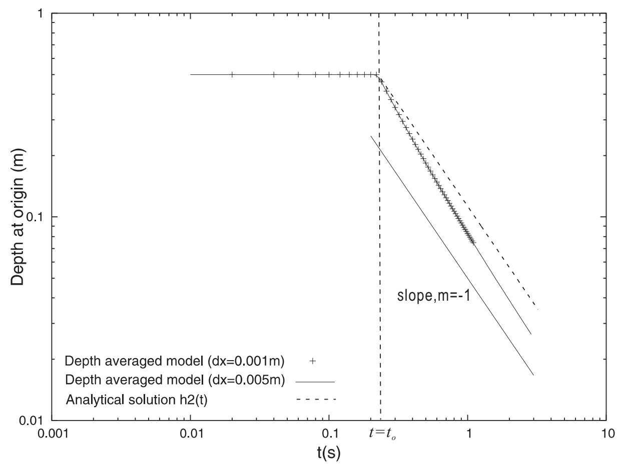

Fig. 7 Temporal variation of depth at the origin h_m for depth averaged model and analytical solution.

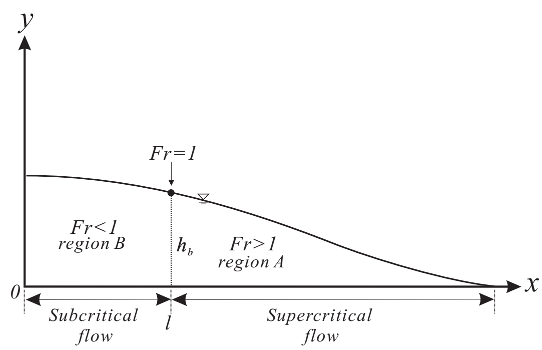

Fig. 8 Temporal variation of depth at the origin h_m for depth averaged model and analytical solution.

4. Conclusion

In this study, the analytical solutions of dam break flow of finite extent are derived by dividing the flow region into 2 regions. The analytical solution of $h_1(t)$

matches the flow profile of the depth averaged model. The analytical solution of $h_2(t)$ also shows satisfactory results although it is not accurately matching the flow profile of the depth averaged model. It is thought that the accuracy of analytical solution of $h_2(t)$ can be further improved by adding higher order terms in the expansion series of flow depth coefficients $a_0(t)$ and $a_2(t)$, as well as the flow velocity coefficients $b_1(t)$. The author plans to carry out further improvement in this aspect. The method presented here in describing the dam break flow of finite-extent has provided a rather different way in analyzing the classical dam break flow problem. It has also provided an in-sights of the flow characteristics in the dam break flow of finite extent as well.

REFERENCES

1) Kokada, T., Hosoda, T. and Miyagawa, T.: Study on a method of obtaining yield values of fresh concrete from slump flow test, *Concrete Lib. of JSCE,* Vol.32, pp.29–41, 1998.
2) Puay, H.T. and Hosoda, T.: Study of characteristics of inertia and viscous flow regions by means of dam break flow with finite volume, *J. App Mech. JSCE,* Vol.10, pp.757–768, 2007.
3) Jain, S.C.: *Open Channel Flow,* John Wiley and Sons, Inc., New York, 2001.
4) Hogg, A.J. and Pritchard, D.: The effect of hydraulics resistance on dam break and other shallow inertial flows, *J. Fluid. Mech.,* Vol.501, pp.179–212, 2004.

(Received April 09, 2009)